

Agent Based Models of Language Competition: Macroscopic descriptions and Order-Disorder transitions

F. Vazquez, X. Castelló and M. San Miguel

IFISC, Institut de Física Interdisciplinària i Sistemes Complexos (CSIC-UIB),
Campus Universitat Illes Balears, E-07122 Palma de Mallorca, Spain

E-mail: federico@ifisc.uib-csic.es

Abstract. We investigate the dynamics of two agent based models of language competition. In the first model, each individual can be in one of two possible states, either using language X or language Y , while the second model incorporates a third state XY , representing individuals that use both languages (bilinguals). We analyze the models on complex networks and two-dimensional square lattices by analytical and numerical methods, and show that they exhibit a transition from one-language dominance to language coexistence. We find that the coexistence of languages is more difficult to maintain in the Bilinguals model, where the presence of bilinguals in use facilitates the ultimate dominance of one of the two languages. A stability analysis reveals that the coexistence is more unlikely to happen in poorly-connected than in fully connected networks, and that the dominance of only one language is enhanced as the connectivity decreases. This dominance effect is even stronger in a two-dimensional space, where domain coarsening tends to drive the system towards language consensus.

1. Introduction

A deep understanding of collective phenomena in Statistical Mechanics is well established in terms of microscopic spin models. Useful macroscopic descriptions of these models in terms of mean field approaches, pair and higher order approximations, and field theories are also well known. Partly inspired by this success, collective social phenomena are being currently studied in terms of microscopic models of interacting agents [1]. Agents, playing here the role of spins, sit in the nodes of a network of social interactions and change their state (social option) according to specified dynamical rules of interaction with their neighbors in the network. A general question addressed is the consensus problem, reminiscent of order-disorder transitions: The aim is to establish ranges of the parameters determining the interaction rules and network characteristics for which the system is eventually dominated by one state or option or, on the contrary, when a configuration of global coexistence is reached [2].

Language competition falls within the context of such social consensus problems: One considers a population of agents that can use either of two languages (two states). The agents change their state of using one or the other language, by interactions with other agents. One is here interested in determining when a state of dominance (or extinction) of one language is reached, or when a state of global language coexistence, with a finite fraction of the two kind of speakers, prevails. A particular and interesting ingredient in this problem is the possibility of a third state associated with bilingual agents, which have been claimed to play an essential role in processes of language contact [3, 4]. A good deal of work along these lines originates in a paper by Abrams and Strogatz [5]. These authors introduced a simple population dynamics model with the aim of describing the irreversible death of many languages around the world [6]. The original Abrams-Strogatz model (ASM) was a macroscopic description based on ordinary differential equations, but a corresponding microscopic agent based model was described in [7]. This model features probabilities to switch languages determined by the local density of speakers of the opposite language, and by two parameters that we call *prestige*, \mathcal{S} and *volatility*, a . Prestige is a symmetry breaking parameter favoring the state associated with one or other language which accounts for the differences in the social status between the two languages in competition. The volatility parameter determines the functional form of the switching probability. It characterizes a property of the social dynamics associated to the inertia of an agent to change its current option, with its neutral value $a = 1$ corresponding to a mechanism of random imitation of a neighbor in the network. Other studies of the ASM account for the effects of geographical boundaries introduced in terms of reaction-diffusion equations [8] or for Lotka-Volterra modifications of the original model [9]. Another different class of models accounts for many languages in competition, with the aim of reproducing the distribution of language sizes in the world [10, 11].

While in the original paper of Abrams and Strogatz [5] the two parameters \mathcal{S} and a were fitted to a particular linguistic data, most subsequent work has focused on

theoretical analysis for the case of symmetrical prestige and neutral volatility. For these parameter values (symmetric \mathcal{S} and $a = 1$) the microscopic ASM coincides with the voter model [12], a paradigmatic spin model of nonequilibrium dynamics [13]. Inspired in the modifications proposed by Minett and Wang of the ASM [14, 15], a microscopic Bilinguals model (BM) which introduces a third (intermediate) state to account for bilingualism has been studied for the case of symmetric \mathcal{S} and $a = 1$ in [16]. In this way, this case is an extension of the original voter model. The emphasis has been in describing the effects of the third state of bilingual agents in the dynamics of language competition as compared with the reference case provided by the voter model. This includes the characterization of the different processes of domain growth [16], and the role of the network topology, like small world networks [16] and networks with mesoscopic community structure [17, 18]. Other studies associated to variations of the voter model dynamics and the addition of intermediate states have also been addressed in [19, 20, 21, 22, 23, 24].

A pending task in the study of this class of models for language competition is, therefore, the detailed analysis of the role of the prestige and volatility in their general dynamical properties. In addition, for the voter model, macroscopic field theory descriptions [25, 26] as well as macroscopic and analytical solutions in different complex networks [27] have been reported, but there is still a lack of useful macroscopic descriptions of these models for arbitrary values of the prestige and volatility parameters. The general aim of this paper is then, to explore the behavior of these models for a wide range of these parameters values, and to derive appropriate macroscopic descriptions that account for the observed order-disorder (language dominance-coexistence) transitions in the volatility-prestige parameter space. In particular, we analyze how the introduction of an intermediate bilingual state affects language coexistence, by comparing the regions of coexistence and one-language dominance of the ASM and BM in the parameter space. In addition, we study how these regions are modified, within the same models, when the dynamics takes place on networks with different topologies.

The paper is organized as follows. In section 2, we introduce and study the Abrams-Strogatz model on fully connected and complex networks. Starting from the microscopic dynamics, we derive ordinary differential equations for the global magnetization (difference between the fraction of speakers of each language) and the interface density (fraction of links connecting opposite-language speakers). We use these equations to analyze ordering and stability properties of the system, that is, whether there is language coexistence or monolingual dominance in the long time limit. In section 3, we introduce and study the Bilinguals model, following an approach similar to the one in section 2. In section 4, we address the behavior of these language competition models and the order-disorder transitions on square lattices. In particular, we build a macroscopic description of the dynamics of the ASM on square lattices by deriving partial differential equations for the magnetization field, that depend on space and time. Finally, in section 5 we present a discussion and a summary of the results.

2. Abrams and Strogatz model

The microscopic agent based version [7, 16] of the model proposed by Abrams and Strogatz [5] considers a population of N individuals sitting in the nodes of a social network of interactions. Every individual can speak two languages X and Y , but it uses only one at a time. In a time step, an individual chosen at random is given the possibility to give up the use of its language and start using the other language. The likelihood that the individual changes language use depends on the fraction of its neighbors using the opposite language. Neighbors are here understood as agents sitting in nodes directly connected by a link of the network. The language switching probabilities are defined as

$$\begin{aligned} P(X \rightarrow Y) &= (1 - \mathcal{S}) \sigma_y^a \quad \text{and} \\ P(Y \rightarrow X) &= \mathcal{S} \sigma_x^a, \end{aligned} \tag{1}$$

where $\sigma_x(\sigma_y)$ is the density of $X(Y)$ neighboring speakers of a given individual, $0 \leq \mathcal{S} \leq 1$ is the *prestige* of language X , and $a > 0$ is the *volatility* parameter. \mathcal{S} controls the asymmetry of language change [$\mathcal{S} > 1/2$ ($\mathcal{S} < 1/2$) favoring language $X(Y)$], whereas a measures the tendency to switch language use. The case $a=1$ is a neutral situation, in which the transition probabilities depend linearly on the local densities. A high volatility regime exists for $a < 1$, with a probability of changing language state above the neutral case, and therefore agents change their state rather frequently. A low volatility regime exists for $a > 1$ with a probability of changing language state below the neutral case with agents having a larger resistance or inertia to change their state.

Having defined the model, we would like to investigate the dynamics and ultimate fate of the population, that is, whether all individuals will agree after many interactions in the use of one language or not. In order to perform an analytical and numerical study of the evolution of the system we consider, in an analogy to spin models, X and Y speakers as spin particles in states $s = -1$ (spin down) and $s = 1$ (spin up) respectively. Thus, the state of the system in a given time can be characterized quite well by two macroscopic quantities: The global magnetization $m \equiv \frac{1}{N} \sum_{i=1}^N S_i$, (S_i with $i = 1, \dots, N$ is the state of individual i in a population of size N), and the density of pairs of neighbors using different languages $\rho \equiv \frac{1}{2N_l} \sum_{\langle ij \rangle} (1 - S_i S_j)/2$, where N_l is the number of links in the network and the sum is over all pair of neighbors. The magnetization measures the balance in the fractions of X and Y speakers ($m = 0$ corresponding to the perfectly balanced case), whereas ρ measures the degree of disorder in the system. The case $|m| = 1$ and $\rho = 0$ corresponds to the totally ordered situation, with all individuals using the same language, while $|m| < 1$ and $\rho > 0$ indicates that the system is disordered, composed by both type of speakers.

The aim is to obtain differential equations for the time evolution of the average values of m and ρ . These equations are useful in the study of the properties of the system, from an analytical point of view. We start by deriving these equations in the case of a highly connected society with no social structure (fully connected network),

that corresponds to the simplified assumption of a “well mixed” population, widely used in population dynamics. We then obtain the equations in a more realistic scenario, when the topology of interactions between individuals is a social complex network. We shall see that the results depend on the particular properties of the network under consideration, reflected in the moments of the degree distribution.

2.1. Fully connected networks

We consider a network composed by N nodes, in which each node has a connection to any other node. In a time step $\delta t = 1/N$, a node i with state s ($s = \pm 1$) is chosen with probability σ_s . Then, according to the transitions (1), i switches its state with probability

$$P(s \rightarrow -s) = \frac{1}{2}(1 - sv) (\sigma_{-s})^a, \quad (2)$$

where σ_{-s} is the density of neighbors of i with state $-s$, that in this fully connected network is equal to the global density of $-s$ nodes. Given that the total number of individuals is conserved we have that $\sigma_- + \sigma_+ = 1$. We define the bias $v \equiv 1 - 2\mathcal{S}$ ($-1 < v < 1$) as a measure of the preference for one of the two languages, with $v > 0$ ($v < 0$) favoring the $s = 1$ ($s = -1$) state. In the case that the switch occurs, the density σ_s is reduced by $1/N$, for which the magnetization $m = \sigma_+ - \sigma_-$ changes by $-2s/N$. Then, the average change in the magnetization can be written as

$$\frac{dm(t)}{dt} = \frac{1}{1/N} \left[\sigma_- P(- \rightarrow +) \frac{2}{N} - \sigma_+ P(+ \rightarrow -) \frac{2}{N} \right]. \quad (3)$$

Using Eq. (2) and expressing the global densities σ_{\pm} in terms of the magnetization, $\sigma_{\pm} = (1 \pm m)/2$, we arrive to

$$\frac{dm(t)}{dt} = 2^{-(a+1)}(1 - m^2) [(1 + v)(1 + m)^{a-1} - (1 - v)(1 - m)^{a-1}]. \quad (4)$$

Equation (4) describes the evolution of a very large system ($N \gg 1$) at the macroscopic level, neglecting finite size fluctuations. This equation for the magnetization is enough to describe the system, given that the density of neighboring nodes in opposite state ρ can be indirectly obtained through the relation

$$\rho(t) = 2\sigma_+(t)\sigma_-(t) = \frac{[1 - m^2(t)]}{2}. \quad (5)$$

2.1.1. Stability Equation (4) has three stationary solutions

$$m_- = -1, \quad m^* = \frac{(1 - v)^{\frac{1}{a-1}} - (1 + v)^{\frac{1}{a-1}}}{(1 - v)^{\frac{1}{a-1}} + (1 + v)^{\frac{1}{a-1}}} \quad \text{and} \quad m_+ = 1. \quad (6)$$

The stability of each of the solutions depends on the values of the parameters a and v . A simple stability analysis can be done by considering a small perturbation ϵ around a stationary solution m_s . For $m_s = m_{\pm}$, we replace m in Eq. (4) by $m = \pm 1 \mp \epsilon$ (with $\epsilon > 0$), and expand to first order in ϵ to obtain

$$\frac{d\epsilon}{dt} = 2^{-a} [(1 \mp v)\epsilon^{a-1} - 2^{a-1}(1 \pm v)] \epsilon. \quad (7)$$

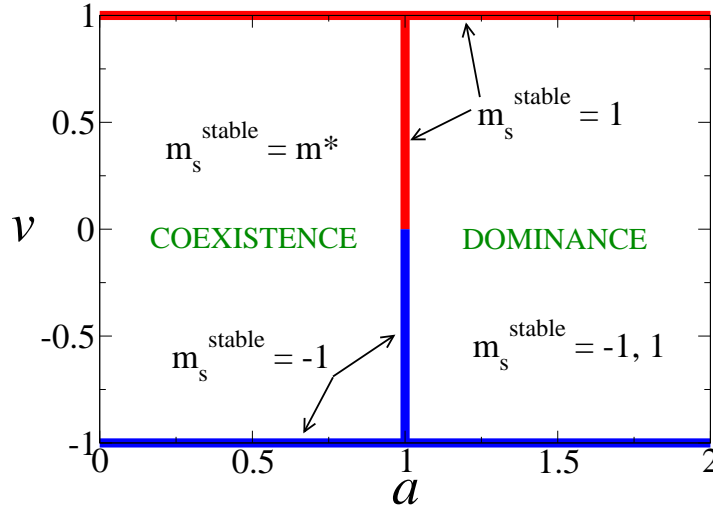


Figure 1. Coexistence and dominance regions of the Abrams-Strogatz model in a fully connected network. For values of the volatility parameter $a > 1$, the stable solutions are those of language dominance, i.e., all individuals using language X ($m_s = -1$) or all using language Y ($m_s = 1$), whereas for $a < 1$ both languages coexist, with a relative fraction of speakers that depends on a and the difference between languages' prestige, measured by the bias v . In the extreme case $v = -1$ ($v = 1$), only language switchings towards X (Y) are allowed, and thus only one dominance state is stable, independent on a .

When $a < 1$, $\epsilon^{a-1} \rightarrow \infty$ as $\epsilon \rightarrow 0$, thus both solutions m_{\pm} are unstable, whereas for $a > 1$, $\epsilon^{a-1} \rightarrow 0$ as $\epsilon \rightarrow 0$, thus m_{\pm} are stable. In the line $a = 1$, m_+ is unstable (stable) for $v < 0$ ($v > 0$), and vice-versa for m_- . The same analysis for the intermediate solution m^* leads to

$$\frac{d\epsilon}{dt} = 2^{-(a+1)}(a-1)(1-m^{*2}) \left[(1+v)(1+m^*)^{a-2} + (1-v)(1-m^*)^{a-2} \right] \epsilon. \quad (8)$$

Then, m^* is unstable (stable) for $a > 1$ ($a < 1$). In Fig. 1 we show the regions of stability and instability of the stationary solutions on the (a, v) plane obtained from the above analysis. We observe a region of coexistence (m^* stable) and one of bistable dominance (m_+ and m_- stable).

The non-trivial stationary solution, m^* , is shown in Fig. 2 as a function of the parameters a and v . For the coexistence regime ($a < 1$), the absolute value of the stable stationary magnetization $|m^*|$ increases with both, $|v|$ and a . When $v \neq 0$ the coexistence solution includes a majority of agents using the language with higher prestige, and the rest of the agents using the language with lower prestige. On the contrary, for the dominance regime ($a > 1$) $|m^*|$ decreases with a and increases with $|v|$.

In order to account for possible finite size effects neglected in Eq. (4) we have run numerical simulations in a fully connected network. We first notice that the solutions $m = \pm 1$ correspond to the totally ordered *absorbing* configurations, that is, once the system reaches those configurations it never escapes from them. This is because, from

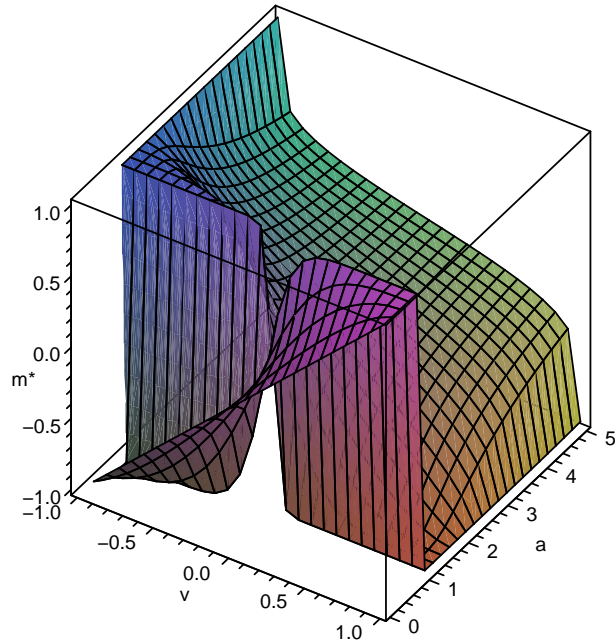


Figure 2. Stationary solution $m^*(a, v)$ for the Abrams-Strogatz model (vertical axis) as a function of the two parameters of the model, a and v (horizontal-plane). See Expression (6). Notice how m^* approaches the values of the two trivial stationary solutions, $m_- = -1$ and $m_+ = +1$ when $a \rightarrow 1$: for $v > 0$, $\lim_{a \rightarrow 1^\pm}(m^*) = \mp 1$. The opposite holds for $v < 0$. The non-trivial stationary solution, m^* , is effectively not defined at $a = 1$, and in this case the system has only two stationary states, m_- and m_+ . The figure illustrates the change of stability of m^* at $a_c = 1$.

the transition probabilities Eq. (2), a node never flips when it has the same state as all its neighbors. Thus, to study the stability of these solutions we have followed a standard approach [13] that consists of adding a defect (seed) to the initial absorbing state and let the system evolve (spreading experiment). If, in average, the defect spreads over the entire system, then the absorbing state is unstable, otherwise if the defect quickly dies out, the absorbing state is stable. For instance, to study the stability of $m = -1$, we started from a configuration composed by $N - 1$ down spins and 1 up spin (seed), that corresponds to a magnetization $m = -1 + 2/N \gtrsim -1$, and we let the system evolve until an absorbing configuration was reached. Whether $m = -1$ is stable or not depends on the values of v and a . If $m = -1$ is unstable, then the seed creates many up spins and spreads over the system, to end in one of the absorbing states. If $m = -1$ is stable, then the initial perturbation dies out, and the system ends in the $m = -1$ absorbing state. The theory of criticality predicts that the survival probability $P(t)$, i.e, the fraction of realizations that have not died up to time t , follows a power-law at the critical point [13], where the stability of the absorbing solution changes. Figure 3 shows that for a fixed value of the bias $v = 0$, $P(t)$ decreases exponentially fast to zero for values of $a > 1$,

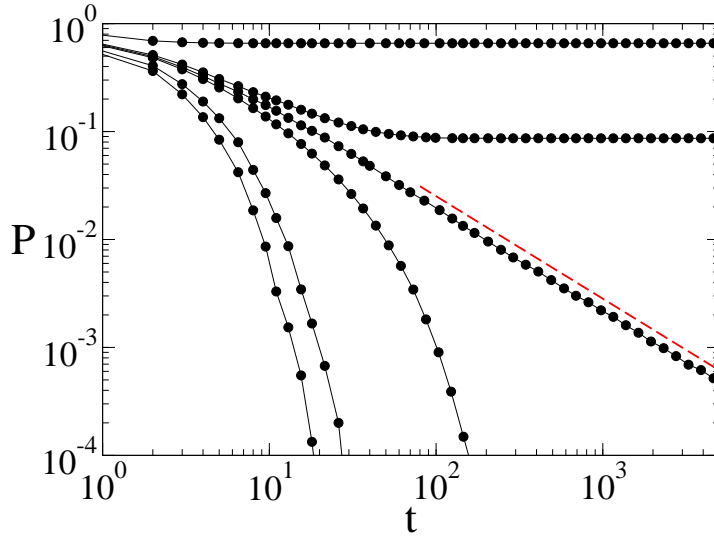


Figure 3. Probability $P(t)$ that the system is still alive at time t , when it starts from a configuration composed by an up spin in a sea of $10^5 - 1$ down spins, endowed with the Abrams-Strogatz dynamics with equivalent languages (bias $v = 0$), on a fully connected network. Different curves correspond to the values $a = 0.90, 0.99, 1.00, 1.01, 1.10$ and 2.0 (from top to bottom). At $a_c \simeq 1.0$, $P(t)$ follows a power law decay with exponent $\delta \simeq 0.95$, indicated by the dashed line.

while it reaches a constant value for $a < 1$. For $a_c \simeq 1.0$, $P(t)$ decays as $P(t) \sim t^{-\delta}$, with $\delta \simeq 0.95$, indicating the transition line from an unstable to a stable solution $m = -1$ as a is increased, in agreement with the previous stability analysis.

Following the same procedure, we have also run spreading experiments to check the stability transition for different values of the bias. For $v = -0.02$ and $v = -0.2$, on a system of size $N = 10^5$, we found the transitions at $a \simeq 1.007$ and $a \simeq 1.052$, respectively. These values are slightly different from the analytical value $a_c \simeq 1.0$, but we have verified that as N is increased, the values become closer to 1.0, in agreement with the stability analysis on infinite large systems.

An alternative and more visual way of studying stability in the mean field limit, is by writing Eq. (4) in the form of a time-dependent Ginzburg-Landau equation

$$\frac{dm(t)}{dt} = -\frac{\partial V_{a,v}(m)}{\partial m}, \quad (9)$$

with potential

$$\begin{aligned} V_{a,v}(m) \equiv 2^{-a} \left\{ -vm - \frac{1}{2}(a-1)m^2 + \frac{v}{6}[2 - (a-1)(a-2)]m^3 \right. \\ \left. + \frac{1}{24}(a-1)[6 - (a-2)(a-3)]m^4 + \frac{v}{10}(a-1)(a-2)m^5 \right. \\ \left. + \frac{1}{36}(a-1)(a-2)(a-3)m^6 \right\}. \end{aligned} \quad (10)$$

$V_{a,v}$ is obtained by Taylor expanding the term in square brackets of Eq. (4) up to 3-rd order in m , and integrating once over m . We assume that higher order terms in the

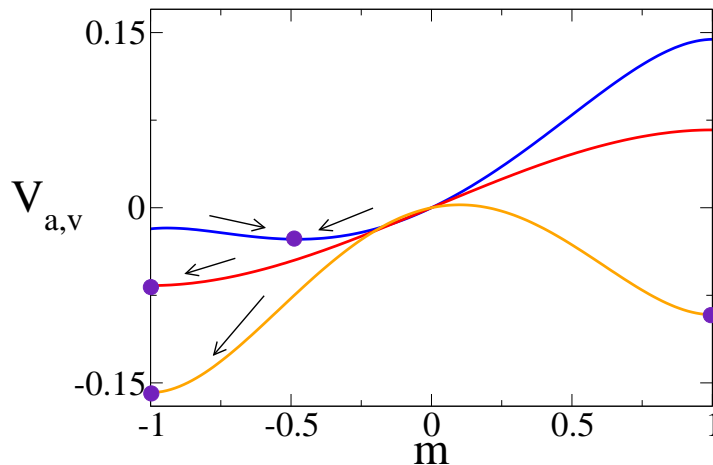


Figure 4. Ginzburg-Landau potential from Eq. (10), for the Abrams-Strogatz model with bias $v = -0.1$ and values of volatility $a = 0.8, 1.0$ and 2.0 (from top to bottom). Arrows show the direction of the system’s magnetization towards the stationary solution (solid circles). For $a = 0.8$ the minimum is around $m \simeq -0.5$, indicating that the system relaxes towards a partially ordered stationary state, while for $a = 1.0$ and 2.0 , it reaches the complete ordered state $m = -1$.

expansion are irrelevant, and the dynamics is well described by an m^6 -potential.

Within this framework, the state of the system, represented by a point $m(t)$ in the magnetization one-dimensional space $-1 < m < 1$, moves “down the potential hill”, trying to reach a local minimum. Therefore, a minimum of $V_{a,v}$ at some point m_s represents a stable stationary solution, given that if the system is moved apart from m_s and then released, it immediately goes back to m_s , whereas a maximum of $V_{a,v}$ represents an unstable stationary solution. As Fig. 4 shows, for $a < 1$ and all values of v , the single-well potential has a minimum at $|m_s| < 1$ ($m_s \simeq -0.5$ for $a = 0.8$ and $v = -0.1$), indicating that the system reaches a partially ordered stable state, with fractions 0.75 and 0.25 of down and up spins, respectively, and a density of opposite-state links $\rho \simeq 0.375$. For $a > 1$, the double-well potential has a minimum at $m = \pm 1$, thus depending on the initial magnetization, the system is driven to one of the stationary solutions $m = \pm 1$, corresponding to the totally ordered configurations in which $\rho = 0$.

This description works well in infinite large systems, where finite size fluctuations are zero. But in finite systems, the absorbing solutions $m = \pm 1$ are the only “truly stationary states”, given that fluctuations ultimate take the system to one of those states. Even for the case $a < 1$, where the minimum is at $|m_s| < 1$, the magnetization fluctuates around m_s for a very long time until after a large fluctuation it reaches $|m| = 1$, and the system freezes.

2.1.2. $a = 1$ case: the voter model For $a = 1$ the ASM becomes equivalent to the voter model. A switching probability proportional to the local density of neighbors in the opposite state is statistically equivalent to adopt the state of a randomly chosen

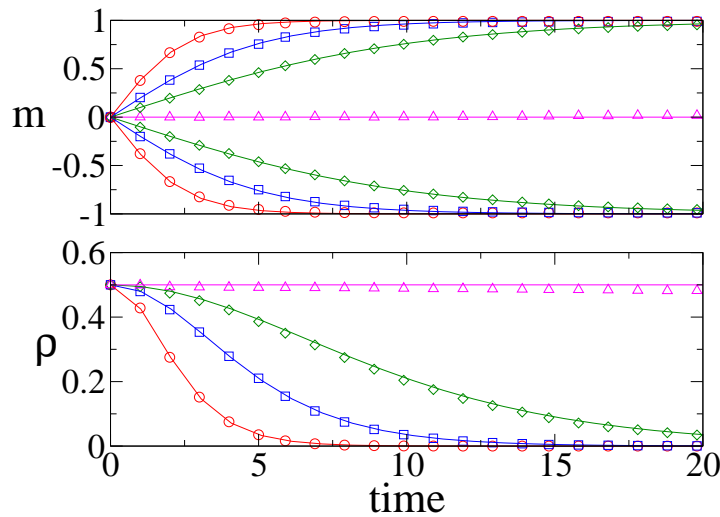


Figure 5. Abrams-Strogatz model on a fully connected network of $N = 1000$ nodes with volatility $a = 1$. Upper panel: Average magnetization m vs time for values of the bias $v = 0.8, 0.4, 0.2, 0.0, -0.2, -0.4$ and -0.8 (from top to bottom). Lower panel: Average density of opposite-state links ρ vs time for $v = 0.0, 0.2, 0.4$ and 0.8 (top to bottom). Open symbols are the results from numerical simulations, while solid lines in the upper and lower panels correspond to the solutions from Eqs. (13) and (14) respectively. Averages are over 100 independent realizations starting from a configuration with a uniform distribution of spins and global magnetization $m(0) = 0$.

neighbor. In this limit of neutral volatility, $a = 1$, Eq. (4) becomes

$$\frac{dm}{dt} = \frac{v}{2}(1 - m^2), \quad (11)$$

whose solution is

$$m(t) = \frac{(1 + m_0)e^{vt} - (1 - m_0)}{(1 + m_0)e^{vt} + (1 - m_0)}, \quad (12)$$

with $m_0 = m(t = 0)$. For a uniform initial condition is $m_0 = 0$, thus

$$m(t) = \tanh(vt/2), \quad (13)$$

and

$$\rho(t) = \frac{1}{2} [1 - \tanh^2(vt/2)]. \quad (14)$$

In Fig. 5 we observe that the analytical solutions from Eqs. (13) and (14) agree very well with the results from numerical simulations of the model, for large enough systems, and they also reproduce the Monte Carlo results found in [7]. This is so, because finite-size fluctuations effects are negligible compare to bias effects, even for a small bias.

When the bias is exactly zero, one obtains that in an infinite large network $dm/dt = 0$, thus m and ρ are conserved. However, in a finite network, fluctuations always lead the system to one of the absorbing states [7]. To find how the system relaxes to the final state, one needs to calculate the evolution of the second moment $\langle m^2 \rangle$ of the magnetization, related to the fluctuations in m , where the symbol $\langle \rangle$ represents

an average over many realizations. This leads to a decay of the average density of opposite-state links of the form (see [27])

$$\langle \rho(t) \rangle = \frac{1}{2} [1 - \langle m^2(t) \rangle] = \langle \rho(0) \rangle e^{-2t/N}. \quad (15)$$

In terms of the potential description of Eq. (9), we observe that when $v \neq 0$, $V_{a,v}$ has only one minimum (see Fig. 4), thus the system has a preference for one of the absorbing states only, whereas if $v = 0$, $V_{a,v} = 0$, and the magnetization is conserved ($m(t) = m(0) = \text{constant}$). In finite systems, even though the average magnetization over many realizations is conserved, the system stills orders in individual realizations by finite size fluctuations.

2.2. Complex networks

In real life, most individuals in a large society interact only with a small number of acquaintances, and they all form a social network of connections, where nodes represent individuals and links between them represent interactions. Thereby, we consider a network of N nodes, with a given degree distribution P_k , representing the fraction of individuals connected to k neighbors, such that $\sum_k P_k = 1$. In order to develop a mathematical approach that is analytically tractable, we assume that the network has no degree correlations, as it happens for instance in Erdős-Renyi [28] and Barabási-Albert scale-free networks [29]. It turns out that dynamical correlations between the states of second nearest-neighbors are negligible in voter models on uncorrelated networks [27, 30]. Thus, taking into account only correlations between first nearest-neighbors allows to use an approach, called *pair approximation*, that leads to analytical results in good agreement with simulations. In this section, we shall use this approximation to build equations for the magnetization and the density of links in opposite state.

In a time step $\delta t = 1/N$, a node i with degree k and state s is chosen with probability $P_k \sigma_s$. Here we assume that the density of nodes in state s within the subgroup of nodes with degree k is independent on k and equal to the global density σ_s . Then, according to transitions (1), i switches its state with probability

$$P(s \rightarrow -s) = \frac{1}{2}(1 - sv) (n_{-s}/k)^a, \quad (16)$$

where we denote by n_{-s} the number of neighbors of i in the opposite state $-s$ ($0 \leq n_{-s} \leq k$) and the bias v is defined as in the previous section. If the switch occurs, the density σ_s is reduced by $1/N$, for which the magnetization $m = \sigma_+ - \sigma_-$ changes by $-2s/N$, while the density ρ changes by $2(k - 2n_{-s})/\mu N$, where $\mu \equiv \sum_k k P_k$ is the average degree of the network. Thus, in analogy to section 2.1, but now plugging the transition probabilities from Eq. (16) into Eq. (3), we write the average change in the magnetization as

$$\frac{dm(t)}{dt} = \sum_k \frac{P_k \sigma_-}{1/N} \sum_{n_+=0}^k B(n_+, k) \frac{(1+v)}{2} \left(\frac{n_+}{k}\right)^a \frac{2}{N}$$

$$- \sum_k \frac{P_k \sigma_+}{1/N} \sum_{n_-=0}^k B(n_-, k) \frac{(1-v)}{2} \left(\frac{n_-}{k}\right)^a \frac{2}{N}, \quad (17)$$

and similarly, the change in the density of links in opposite state as

$$\begin{aligned} \frac{d\rho(t)}{dt} = & \sum_k \frac{P_k \sigma_-}{1/N} \sum_{n_+=0}^k B(n_+, k) \frac{(1+v)}{2} \left(\frac{n_+}{k}\right)^a \frac{2(k-2n_+)}{\mu N} \\ & + \sum_k \frac{P_k \sigma_+}{1/N} \sum_{n_-=0}^k B(n_-, k) \frac{(1-v)}{2} \left(\frac{n_-}{k}\right)^a \frac{2(k-2n_-)}{\mu N}. \end{aligned} \quad (18)$$

We denote by $B(n_s, k)$, the probability that a node of degree k and state $-s$ has n_s neighbors in the opposite state s . Defining the a -th moment of $B(n_s, k)$ as

$$\langle n_s^a \rangle_k \equiv \sum_{n_s=0}^k B(n_s, k) n_s^a,$$

we arrive to the equations

$$\frac{dm(t)}{dt} = \sum_k \frac{P_k}{2k^a} [(1+v)(1-m)\langle n_+^a \rangle_k - (1-v)(1+m)\langle n_-^a \rangle_k], \quad (19)$$

$$\begin{aligned} \frac{d\rho(t)}{dt} = & \sum_k \frac{P_k}{2\mu k^a} \left\{ (1+v)(1-m) \left[k\langle n_+^a \rangle_k - 2\langle n_+^{(1+a)} \rangle_k \right] \right. \\ & \left. + (1-v)(1+m) \left[k\langle n_-^a \rangle_k - 2\langle n_-^{(1+a)} \rangle_k \right] \right\}. \end{aligned} \quad (20)$$

2.2.1. $a = 1$ case: the voter model In order to develop an intuition about the temporal behavior of m and ρ from Eqs. (19) and (20), we first analyze the simplest and non-trivial case $a = 1$, that corresponds to the voter model on complex networks. A rather complete analysis of the time evolution and consensus times of this model on uncorrelated networks, for the symmetric case $v = 0$, can be found in [27]. Following a similar approach, here we study the general situation in which the bias v takes any value. To obtain closed expressions for m and ρ , we consider that the system is “well mixed”, in the sense that the different types of links are uniformly distributed over the network. Therefore, we assume that the probability that a link picked at random is of type $+ -$ is equal to the global density of $+ -$ links ρ . Then, $B(n_s, k)$ becomes the binomial distribution with

$$P(-s|s) = \rho/2\sigma_s \quad (21)$$

as the single event probability that a first nearest-neighbor of a node with state s has state $-s$. Here, we use the fact that in uncorrelated networks dynamical correlations between the states of second nearest-neighbors vanish (pair approximation). $P(-s|s)$ is calculated as the ratio between the total number of links $\rho\mu N/2$ from nodes in state s to nodes in state $-s$, and the total number of links $N\sigma_s\mu$ coming out from nodes in

state s . Taking $a = 1$ in Eqs. (19) and (20), and replacing the first and second moments of $B(n_{-s}, k)$ by

$$\begin{aligned}\langle n_{-s} \rangle &= P(-s|s)k, \\ \langle n_{-s}^2 \rangle &= P(-s|s)k + P(-s|s)^2k(k-1),\end{aligned}$$

leads to the following two coupled closed equations for m and ρ

$$\frac{dm(t)}{dt} = v\rho \quad (22)$$

$$\frac{d\rho(t)}{dt} = \frac{\rho}{\mu} \left\{ \mu - 2 - \frac{2(\mu-1)(1+vm)\rho}{(1-m^2)} \right\}. \quad (23)$$

For $v = 0$, the above expressions agree with the ones of the symmetric voter model [27]. For the asymmetric case $v \neq 0$, we have checked numerically that the only stationary solutions are $(m = 1, \rho = 0)$ for $v > 0$ and $(m = -1, \rho = 0)$ for $v < 0$, that correspond to the fully ordered state, as we were expecting. Even though an exact analytical solution of Eqs. (22) and (23) is hard to obtain, we can still find a solution in the long time limit, assuming that ρ decays to zero as

$$\rho = A e^{-t/2\tau(v)}, \quad \text{for } t \gg 1, \quad (24)$$

where A is a constant given by the initial state and $\tau(v)$ is another constant that depends on v , and quantifies the rate of decay towards the solutions $m = 1$ or $m = -1$. To calculate the value of τ we first replace the ansatz from Eq. (24) into Eq. (22), and solve for m with the boundary conditions $m(\rho = 0) = 1$ and -1 , for $v > 0$ and $v < 0$, respectively. We obtain

$$m = \begin{cases} 1 - 2v\tau\rho & \text{if } v > 0; \\ -1 - 2v\tau\rho & \text{if } v < 0. \end{cases} \quad (25)$$

Then, to first order in ρ is

$$(1 - m^2) = \begin{cases} 4v\tau\rho & \text{if } v > 0; \\ -4v\tau\rho & \text{if } v < 0. \end{cases} \quad (26)$$

Replacing the above expressions for m and $(1 - m^2)$ into Eq. (23), and keeping only the leading order terms, we arrive to the following expression for τ

$$\tau(v) = \begin{cases} \frac{\mu-1-v}{2v(\mu-2)} & \text{if } v > 0; \\ \frac{1-\mu-v}{2v(\mu-2)} & \text{if } v < 0. \end{cases} \quad (27)$$

Finally, the magnetization for long times behave as

$$m = \begin{cases} 1 - \frac{(\mu-1-v)A}{\mu-2} \exp\left[-\frac{v(\mu-2)}{\mu-1-v}t\right] & \text{if } v > 0; \\ -1 + \frac{(\mu-1+v)A}{\mu-2} \exp\left[\frac{v(\mu-2)}{\mu-1+v}t\right] & \text{if } v < 0, \end{cases} \quad (28)$$

whereas the density of opposite state links decays as

$$\rho = A \exp\left[-\frac{|v|(\mu-2)}{\mu-1-|v|}t\right]. \quad (29)$$

Using the expression for $\tau(S)$ from Eq. (27) in Eq. (26), and taking the limit $v \rightarrow 0$, we find that $\rho(t) = \frac{(\mu-2)}{2(\mu-1)} [1 - m(t)^2]$, in agreement with previous results of the voter model on uncorrelated networks [27]. By taking $\mu = N - 1 \gg 1$ in Eqs. (28) and (29), we recover the expressions for m and ρ on fully connected networks [Eqs. (13) and (14), respectively], in the long time limit. This result means that the evolution of m and ρ in the biased voter model on uncorrelated networks is very similar to the mean-field case, with the time rescaled by the constant τ that depends on the topology of the network, expressed by the mean connectivity μ . From the above equations we observe that the system reaches the dominance state $\rho = 0$ in a time of order τ . For the special case $v = 0$, τ diverges, thus Eqs. (28) and (29) predict that both m and ρ stay constant over time. However, as mentioned in section 2.1.2, finite-size fluctuations drive the system to the absorbing state ($\rho = 0, |m| = 1$). Taking fluctuations into account, one finds that the approach to the final state is described by the decay of the average density ρ [27]

$$\langle \rho(t) \rangle = \frac{(\mu - 2)}{2(\mu - 1)} e^{-2t/T}, \quad (30)$$

where $T \equiv \frac{(\mu-1)\mu^2 N}{(\mu-1)\mu_2}$, depends on the system size N , and the first and second moments, μ and μ_2 respectively, of the network.

2.2.2. Stability analysis As in fully connected networks, we assume that Eq. (19) for the magnetization has three stationary solutions. Indeed, we have numerically verified that for different types of networks there is, apart from the trivial solutions $m = 1, -1$, an extra non-trivial stationary solution $m = m^*$. Due to the rather complicated form of Eq. (19), we try to study the stability of the solutions in an approximate way, and find a qualitative picture of the stability diagram in the (a, v) plane. For the general case in which a and v take any values, we assume, as in the voter model case, that $B(n_-, k)$ is a binomial probability distribution with single event probabilities given by Eq. (21). Then, the explicit form for the a -th moment of $B(n, k)$ is

$$\langle n_s^a \rangle = \sum_{n_s=0}^k n^a C_{n_s}^k \left(\frac{\rho}{2\sigma_{-s}} \right)^{n_s} \left(1 - \frac{\rho}{2\sigma_{-s}} \right)^{k-n_s}. \quad (31)$$

We also assume that, as it happens for the voter model case $a = 1$ [see Eq. (26)], ρ and m are related by $\rho(t) \simeq \frac{q}{2} [1 - m^2(t)]$, where q is a constant that depends on a and v . We note that this relation satisfies the fully-ordered-state condition $\rho = 0$ when $|m| = 1$. We shall see that the exact functional form of $q = q(a, v)$ is irrelevant for the stability results, as long as $q > 0$. To simplify calculations even more, we consider that the network is a degree-regular random graph with degree distribution $P_k = \delta_{k,\mu}$, that is, all nodes have exactly μ neighbors chosen at random. Then, replacing the above expression for the moments into Eq. (19), and substituting ρ by the approximate value $\frac{q}{2} [1 - m^2]$, we arrive to the following closed equation for m

$$\frac{dm}{dt} = \frac{(1 - m^2)}{2\mu^a} \sum_{n=0}^{\mu} C_n^{\mu} n^a \left(\frac{q}{2} \right)^n \left\{ (1 + v)(1 + m)^{n-1} [1 - p(1 + m)]^{\mu-n} \right.$$

$$- (1 - v)(1 - m)^{n-1} [1 - p(1 - m)]^{\mu-n} \}, \quad (32)$$

where mute indices n_- and n_+ were replaced by the index n . To check the stability of $m = 1$, we take $m = 1 - \epsilon$ in Eq. (32), and expand it to first order in ϵ . We obtain after some algebra

$$\frac{d\epsilon}{dt} = \frac{\mu^{-a}}{2} (\langle n \rangle_q + \langle n^a \rangle_q) [\mathcal{V}_1(a) - v] \epsilon, \quad (33)$$

where the symbols $\langle \cdot \rangle_q$ represent the moments of a Binomial distribution with probability q , and the bias function $\mathcal{V}_1(a)$ is defined as

$$\mathcal{V}_1(a) = \frac{\langle n \rangle_q - \langle n^a \rangle_q}{\langle n \rangle_q + \langle n^a \rangle_q}. \quad (34)$$

Then, for a fixed value of a the solution $m = 1$ is stable (unstable), when v is larger (smaller) than $\mathcal{V}_1(a)$. The shape of the function $\mathcal{V}_1(a)$ can be guessed using that for a larger (smaller) than 1, the moment $\langle n^a \rangle$ is larger (smaller) than $\langle n \rangle$. Then $\mathcal{V}_1(a)$ goes to $(\langle n \rangle - 1)/(\langle n \rangle + 1) \lesssim 1$ and -1 as a approaches to 0 and ∞ , respectively. Also $\mathcal{V}_1(a) = 0$, for $a = 1$. With a similar stability analysis we obtained that $m = -1$ is stable (unstable) for the points (a, v) below (above) the transition line $\mathcal{V}_{-1}(a) = -\mathcal{V}_1(a)$, while $m = m^*$ is stable in the region where both $m = -1$ and $m = 1$ are unstable. In Fig. 6 we show a picture that summarizes the stability regions defined by the transition lines $\mathcal{V}_1(a)$ and $\mathcal{V}_{-1}(a)$. These lines were obtained by integrating numerically the two coupled Eqs. (19) and (20), with the moments defined in Eq. (31), and finding the points (a, v) where the stationary solutions $m = 1, -1$ became unstable. We considered two degree-regular random graphs with degrees $\mu = 3$ [solid lines $\mathcal{V}_1^3(a)$ and $\mathcal{V}_{-1}^3(a)$] and $\mu = 10$ [dashed-lines $\mathcal{V}_1^{10}(a)$ and $\mathcal{V}_{-1}^{10}(a)$], thus we took $P_k = \delta_{k,\mu}$ in the equations. For clarity, only the stable solutions are labeled in the picture. We observe that as the degree of the network increases, the coexistence region expands and approaches to the corresponding region $a < 1$ on fully connected networks.

In order to give numerical evidence, from Monte Carlo simulations, of the different phases and transition lines predicted in Fig. 6, we have run spreading experiments as explained in section 2.1, for a degree-regular random graph (DRRG) with degree $\mu = 3$ and $N = 10^5$ nodes, and tested the stability of the homogeneous solutions $m = \pm 1$. We first set the bias in $v = 0$ and, by varying a , we obtained a transition at $a_c \simeq 1.0$ from dominance to coexistence, as a is decreased: in the dominance region the survival probability $P(t)$ decays exponentially fast to zero, indicating that $m = 1$ is stable, while in the coexistence region $P(t)$ reaches a constant value larger than zero, showing that $m = 1$ is unstable (not shown). This transition is the same as the one in fully connected networks (FCN) (Fig. 3). We then repeated the experiment with $v = -0.2$, whose results are summarized in Fig. 7, where we show $P(t)$ for different values of a . Increasing a from 0, which corresponds to the coexistence regime ($m = \pm 1$ are unstable solutions, and m^* is stable), we show in Fig. 7(a) how in a DRRG $m = -1$ changes from unstable to stable at a value $0.25 < a < 0.3$, as $P(t)$ starts to decay to zero. This corresponds to crossing the line \mathcal{V}_{-1}^3 in the horizontal direction (see Fig. 6), and entering

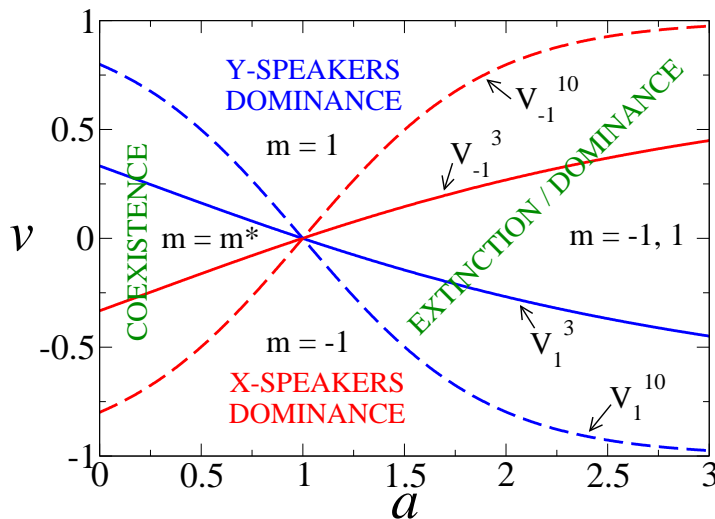


Figure 6. Stability diagram for the Abrams-Strogatz model on a degree-regular random graph, obtained by numerical integration of Eqs. (19), (20) and (31). The solution $m = 1$ is stable above the line \mathcal{V}_1 , while the solution $m = -1$ is stable below the line \mathcal{V}_{-1} . Solid and dashed lines correspond to graphs with degrees $\mu = 3$ and $\mu = 10$ respectively. In the coexistence region, where the stable solution is m^* , the system is composed by both type of users, while in the dominance region, users of either one or the other language prevail, depending on the initial state. We observe that the region of coexistence is reduced, compared to the model on fully connected networks (Fig. 1), and that there are also two single-dominance regions where always the same language dominates.

the monostable region where there exist only two solutions, $m = -1$ stable, and $m = +1$ unstable (m^* becomes equal to -1 along the transition line \mathcal{V}_{-1}^3). In Fig. 7(b) we observe how in a DRRG $m = +1$ becomes stable at a value $1.80 < a < 1.85$. This corresponds to crossing the line \mathcal{V}_1^3 (see Fig. 6) and entering to the dominance region, where both $m = \pm 1$ are stable. Notice that for $a = 1.80$, $P(t)$ first curves up and then it quickly decays to zero at a time $t \simeq 4000$. This means that a finite fraction of realizations starting from a system with a single down spin took, in average, a mean time $t \simeq 4000$ to end up in a configuration with all down spins, showing that $m = -1$ is a stable solution. This supports our claim that in the monostable region there exist only two solutions, $m = -1$ stable, and $m = +1$ unstable. These results confirm the existence of a quite broad single-dominance region in DRRG ($0.30 \lesssim a \lesssim 1.85$ for $v = -0.2$ and $\mu = 3$), in agreement with the stability diagram obtained in Fig. (6), while this region seems to be absent in FCN. Indeed, Fig. 7(c) shows how this unstable-stable transition happens in a FCN at a value $0.93 < a < 1.07$, in agreement with the transition line $a_c \simeq 1.0$ in FCN. Here, both $m = \pm 1$ gain stability at the same point, and the system enters to the dominance region (see Fig 1).

In summary, we find that, compared to the fully connected case, the region of coexistence is shrunk for $v \neq 0$, as there appear two regions where only one solution is stable. These regions also reduce part of the dominance region. The effect of the bias

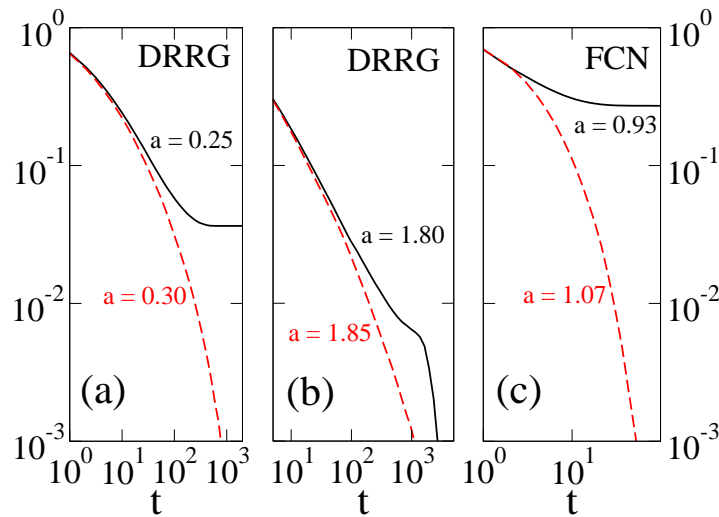


Figure 7. Spreading experiments: probability $P(t)$ that the system is still alive at time t in the Abrams-Strogatz model with bias $v = -0, 2$ and various values of volatility a , showing the stability of the solutions $m = 1, -1$. Dashed curves decay quickly to zero, indicating that the solution is stable while solid curves represent unstable solutions. (a) Degree-regular random graph (DRRG). Stability of the solution $m = -1$: $a = 0.25$ (solid curve), $a = 0.30$ (dashed curve). (b) Degree-regular random graph (DRRG). Stability of the solution $m = +1$: $a = 1.80$ (solid curve), $a = 1.85$ (dashed curve). (c) Fully connected network (FCN). Stability of the solutions $m = \pm 1$: $a = 0.93$ (solid curve), $a = 1.07$ (dashed curve). All curves correspond to an average over 10^5 independent realizations on networks with $N = 10^5$ nodes.

is shown to be more important in DRRGs with low connectivity μ and, as a general result, coexistence becomes harder to achieve in sparse networks.

3. Bilinguals Model

This model can be regarded as an extension of the Abrams-Strogatz model in which, besides monolingual users X and Y , there is a third class of individuals that use both languages, that is, bilingual users labeled with state Z . A monolingual X (Y) becomes a bilingual with a rate depending on the number of its neighbors that are monolinguals Y (X), while direct transitions from one class of monolingual to the other are forbidden. This reflects the fact that individuals that use one language only, are forced to start using both languages if they want to have a conversation with monolingual users of the opposite language. For a similar reason, the transition from a bilingual Z to a monolingual X (Y) depends on the number of neighbors using language X (Y), which includes bilingual agents. Thus, the transition probabilities between states are given by

$$\begin{aligned} P(X \rightarrow Z) &= (1 - \mathcal{S}) \sigma_y^a, \\ P(Z \rightarrow Y) &= (1 - \mathcal{S}) (1 - \sigma_x)^a, \\ P(Y \rightarrow Z) &= \mathcal{S} \sigma_x^a, \end{aligned}$$

$$P(Z \rightarrow X) = \mathcal{S}(1 - \sigma_y)^a, \quad (35)$$

where σ_x , σ_y and σ_z are the densities of neighboring speakers in states X , Y and Z respectively, and \mathcal{S} is the prestige of language X .

As in the ASM, it is convenient to consider monolinguals X and Y , as particles with opposite spins -1 and 1 respectively. Bilinguals are considered as spin-0 particles because they are a combination of the two opposite states. Given that the model is invariant under the interchange of -1 and 1 particles, the system is better described using the global magnetization $m \equiv \sigma_+ - \sigma_-$ and the density of bilinguals σ_0 , where $\sigma_-, \sigma_0, \sigma_+$, are the global densities of nodes in states $-1, 0$ and 1 , respectively. Another alternative could be the use of the density of connections between different states $\rho \equiv 2\sigma_- \sigma_+ + 2\sigma_- \sigma_0 + 2\sigma_+ \sigma_0$, but numerical simulations show that ρ and σ_0 are proportional. We now study the evolution of the system on fully connected and complex networks, by writing equations for m and σ_0 .

3.1. Fully connected networks

In the fully connected case, the local densities of neighbors in the different states agree with the global densities $\sigma_-, \sigma_0, \sigma_+$, thus, using the transition probabilities Eqs. (35), the rate equations for σ_- and σ_+ can be written as

$$\frac{d\sigma_-}{dt} = \frac{(1-v)}{2}\sigma_0(1-\sigma_+)^a - \frac{(1+v)}{2}\sigma_- \sigma_+^a, \quad (36)$$

$$\frac{d\sigma_+}{dt} = \frac{(1+v)}{2}\sigma_0(1-\sigma_-)^a - \frac{(1-v)}{2}\sigma_+ \sigma_-^a, \quad (37)$$

where $v \equiv 1 - 2\mathcal{S}$ is the bias. The rate equations for $m = \sigma_+ - \sigma_-$ and $\sigma_0 = 1 - \sigma_+ - \sigma_-$ can be derived from the above two equations, and by making the substitutions $\sigma_s = (1 - \sigma_0 + s m)/2$, with $s = \pm 1$. We obtain

$$\begin{aligned} \frac{dm}{dt} = 2^{-(2+a)} \left\{ 2\sigma_0 [(1+v)(1+\sigma_0+m)^a - (1-v)(1+\sigma_0-m)^a] \right. \\ \left. + (1+v)(1-\sigma_0-m)(1-\sigma_0+m)^a - (1-v)(1-\sigma_0+m)(1-\sigma_0-m)^a \right\} \end{aligned} \quad (38)$$

and

$$\begin{aligned} \frac{d\sigma_0}{dt} = 2^{-(2+a)} \left\{ -2\sigma_0 [(1+v)(1+\sigma_0+m)^a + (1-v)(1+\sigma_0-m)^a] \right. \\ \left. + (1+v)(1-\sigma_0-m)(1-\sigma_0+m)^a + (1-v)(1-\sigma_0+m)(1-\sigma_0-m)^a \right\}. \end{aligned} \quad (39)$$

Equations (38) and (39) are difficult to integrate analytically, but an insight on its qualitatively behavior can be obtained by studying the stability of the stationary solutions with a and v . As in the ASM, we expect that, for a given v , an order-disorder transition appears at some value a_c of the volatility parameter, where the stability of the stationary solutions changes. If a is small, then flipping rates are high, thus we expect the system to remain in an active disordered state, while for large enough values of a spins tend to be aligned, thus the system should ultimately reach full order. We now calculate the transition point for the symmetric case $v = 0$, and then find an approximate solution for the linear case $a = 1$.

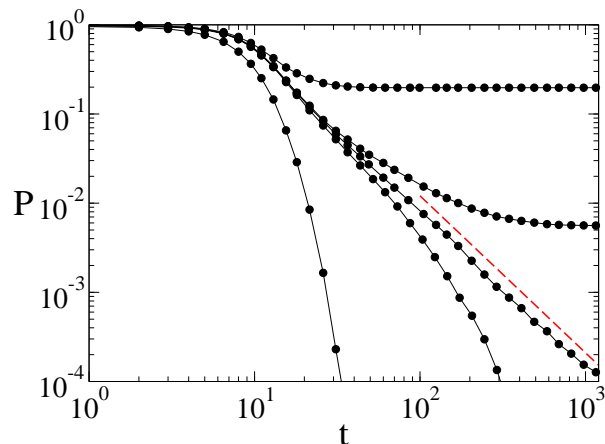


Figure 8. Spreading experiments: probability $P(t)$ that the system is still alive at time t in the Bilinguals model on a fully connected network, obtained from the same spreading experiments and parameters ($v = 0$, $N = 10^5$) as described in Fig. 3 for the Abrams-Strogatz model. The curves correspond to volatilities $a = 0.600, 0.618, 0.620, 0.622$ and 0.700 , (top to bottom). $P(t)$ decays as $t^{-\delta}$ at the transition point 0.620 (close to the theoretical value $a_{fc} \simeq 0.63$), with $\delta \simeq 1.76$, indicated by the dashed line.

3.1.1. Transition point for $v = 0$ In the symmetric case $v = 0$ one can easily verify that the points $(m = \pm 1, \sigma_0 = 0)$ in the (m, σ_0) plane are two stationary solutions of Eqs. (38) and (39). But there is also a third non-trivial stationary solution $(m = 0, \sigma_0 = \sigma_0^*)$, where σ_0^* satisfies

$$2\sigma_0^*(1 + \sigma_0^*)^a - (1 - \sigma_0^*)^{(1+a)} = 0. \quad (40)$$

By doing a small perturbation around $(0, \sigma_0^*)$ in the σ_0 direction, one finds from Eq. (39) that the point $(0, \sigma_0^*)$ is stable for all values of a . Instead, the stability in the m direction changes at some value a_{fc} (fc stands for fully connected). Replacing m by $\epsilon \ll 1$ and σ_0 by σ_0^* in Eq. (38), one arrives to the following relation that σ_0^* and a_{fc} hold when the stability changes

$$2a_{fc}\sigma_0^*(1 + \sigma_0^*)^{(a_{fc}-1)} + (a_{fc} - 1)(1 - \sigma_0^*)^{a_{fc}} = 0. \quad (41)$$

Combining Eqs. (40) and (41), one arrives to the following closed equation for a_{fc}

$$a_{fc} \ln \left(\frac{1 - a_{fc}}{a_{fc}} \right) = \ln \left(\frac{2a_{fc} - 1}{1 - a_{fc}} \right), \quad (42)$$

whose solution is $a_{fc} \simeq 0.63$. Then, assuming that the transition point does not depend on v for FCN, as it happens in the ASM, we find that the (a, v) plane is divided into two regions. In the region $a < a_{fc}$, the stable solution is $(0, \sigma_0^*)$, representing a stable mix of the three kinds of individuals, while in the region $a > a_{fc}$, the stable solutions $(\pm 1, 0)$ indicate the ultimate dominance of one of the languages. By performing spreading experiments we estimated that the transition point for a network of $N = 10^5$ nodes is around $a = 0.62$ (see Fig. 8), and we observed that this value approaches to the analytical

one $a_{fc} \simeq 0.63$ as N increases. We have also checked numerically the transition point when there is a bias ($v \neq 0$), that is, when the two languages are not equivalent. In this case we found a transition around $a = 0.675$ for a bias $v = -0.2$ and $N = 10^5$ nodes, what represents a small deviation from a_{fc} . However this difference is similar to the one found for the ASM in Section 2.1.1 with the same system size. Therefore, we assume that this discrepancy is again due to finite size effects and, in the thermodynamic limit, the transition should be at a_{fc} , for any value of v .

We note that the transition point $a_{fc} \simeq 0.63$ is smaller than the corresponding value $a_c \simeq 1.0$ for the ASM, thus the region for coexistence is reduced in the BM. This has a striking consequence. Suppose that there is population with individuals that can use only one of two languages at a time, and it is characterized by a volatility $a = 0.8$, that allows the stable coexistence of the two languages. If now the behavior of the individuals is changed, so that they can use both languages before they start using the opposite language, the population loses the coexistence and finally approaches to a state with the complete dominance of one language. In other words, within these models, bilinguals in use hinder language coexistence.

3.1.2. AB Model: Neutral volatility and symmetric case For $a = 1$ and $v = 0$, Eqs. (38) and (39) are reduced to

$$\frac{dm}{dt} = \frac{1}{2}\sigma_0 m, \quad (43)$$

$$\frac{d\sigma_0}{dt} = \frac{1}{4}(1 - m^2 - 4\sigma_0 - \sigma_0^2). \quad (44)$$

The three stationary solutions are $(m, \sigma_0) = (-1, 0)$; $(1, 0)$ and $(0, \sqrt{5} - 2)$. Given that the above equations are difficult to integrate analytically, we try an approximate solution by assuming that the density of bilinguals is proportional to the interface density ρ , something observed in our simulations, and already found in [16] for the *AB-model* (equivalent to the BM in the case $v = 0$ and $a = 1$). Bilinguals are at the interface between monolinguals, for all the networks studied. Then we write $\sigma_0 \simeq \alpha\rho$, where α is a constant and $\rho = 2\sigma_-\sigma_+ + 2\sigma_0(\sigma_- + \sigma_+) = \frac{1}{2}[(1 - \sigma_0)^2 - m^2] + 2\sigma_0(1 - \sigma_0)$, from where we obtain that m can be expressed in terms of σ_0 as $m^2 = (1 - \sigma_0)^2 + 4\sigma_0(1 - \sigma_0) - 2\sigma_0/\alpha$. Replacing this expression for m^2 into Eq. (44), we obtain the following equation for σ_0

$$\frac{d\sigma_0}{dt} = \frac{\sigma_0}{2}\left(-3 + \frac{1}{\alpha} + \sigma_0\right). \quad (45)$$

We have checked by numerical simulations that $\alpha > 1/3$, then the solution of the above equation in the long time limit is $\sigma_0 \sim e^{(-3+1/\alpha)t/2}$. Therefore, σ_0 and $|m|$ approach to 0 and 1, respectively, and the system reaches full order exponentially fast.

3.2. Complex networks

We now consider the model on complex networks. Following the same approach as in Section 2.2, it is possible to write down a set of nine coupled differential equations: three for the densities σ_- , σ_0 and σ_+ of node states, and six for the densities ρ_{--} , ρ_{-0} , ρ_{+0} , ρ_{+-} , ρ_{+0} and ρ_{++} of different types of links. However, due to the complexity of these equations, we have limited our study to the investigation of the stability regions through Monte Carlo simulations. We found that in a degree-regular random graph with mean degree $\mu = 3$, the stability diagram is qualitatively similar to the one in Fig. 6 for the ASM, where the coexistence region corresponds to stationary states with a mix of the three types of speakers. Also, the coexistence-dominance transition point for $v = 0$ is at $a_{cn} \simeq 0.3$ (*cn* stands for complex networks). For $v = -0.02$, a monostable region appears for $0.2 \lesssim a \lesssim 0.4$, while this region becomes wider for $v = -0.2$ ($0 \lesssim a \lesssim 1.4$). We have also observed that the coexistence region disappears for $|v| \geq 0.2$. Therefore, in the BM, the region for coexistence also shrinks as the connectivity of the network decreases (going from fully connected to complex networks with low degree), but on top of that, there exists a shift of the critical value from $a_{fc} \simeq 0.63$ (fully connected networks) to $a_{cn} \simeq 0.3$ (degree-regular random graphs). In summary, compared to the ASM, the overall effect of the inclusion of bilingual agents is that of a large reduction of the region of coexistence.

4. Square lattices

Dynamical properties of the ASM and BM in square lattices can be explored for different initial conditions, system sizes, and values of the prestige and volatility parameters, through a simulation applet available online [31]. It turns out that the behavior of these models in square lattices is very different to their behavior in fully connected or complex networks. On the one hand, the mean distance between two sites in the lattice grows linearly with the length of the lattice side L , thus a spin only “feels” the spins that are in its near neighborhood, and therefore the mean-field approach that works well in fully connected networks gives poor results in lattices. On the other hand, correlations between second, third and higher order nearest-neighbors are important in lattices, what causes the formation of same-spin domains, unlike in random networks where correlations to second nearest-neighbors are already negligible. Thus, pair approximation does not provide a good enough description of the dynamics in lattices either, and one is forced to implement higher order approximations (triplets, quadruplets, etc), that lead to a coupled system of many equations, impossible to solve analytically. Due to the fact that the mean-field and pair approximations, that use global quantities such as the magnetization and the density of opposite-state links to describe the system, do not give good results in lattices, we follow here a different approach to obtain a macroscopic description. This approach, also developed in [26] for general nonequilibrium spin models consists in deriving a macroscopic equation for the

evolution of a continuous space dependent spin field. Within this approach it is possible to describe coarsening processes, that is, processes of growth of local linguistic domains caused by the motion of linguistic boundaries (interface motion). In particular, one can explain whether the system orders or not, or if the ordering is curvature driven (interface motion due to surface tension reduction) or noise driven (without surface tension).

We focus here on the ASM, but this macroscopic description can also be applied for systems with three states, as the BM (see [24]). Given that neighboring spins tend to be aligned -due to the ferromagnetic nature of the interactions-, and also correlations between spins reinforce the alignment between far neighbors, the dynamics is characterized by the formation of same-spin domains. Starting from a well-mixed system with up and down spins randomly distributed over the lattice, after a small transient, if we look at the lattice from far we see domains growing and shrinking slowly with time, and we can interpret this dynamics at the coarse-grained level as the evolution of a continuous *spin field* ϕ over space and time. Then, we define by $\phi_{\mathbf{r}}(t)$ the spin field at site \mathbf{r} at time t , which is a continuous representation of the spin at that site ($-1 < \phi < 1$), also interpreted as the average value of the spin over many realizations of the dynamics. Thus, we assume that there are Ω spin particles at each site of the lattice, and we replace $\phi_{\mathbf{r}}(t)$ by the average spin value $\phi_{\mathbf{r}}(t) \rightarrow \frac{1}{\Omega} \sum_{j=1}^{\Omega} S_{\mathbf{r}}^j$, where $S_{\mathbf{r}}^j$ is the spin of the j -th particle inside site \mathbf{r} . Within this formulation, the dynamics is the following. In a time step of length $\delta t = 1/\Omega$, a site \mathbf{r} and a particle from that site are chosen at random. The probability that the chosen particle has spin $s = \pm 1$ is equal to the fraction of \pm spins in that site $(1 \pm \phi_{\mathbf{r}})/2$. Then the spin flips with probability

$$P(s \rightarrow -s) = \frac{1}{2}(1 - sv) \left(\frac{1 - s\psi_{\mathbf{r}}}{2} \right)^a, \quad (46)$$

where $\psi_{\mathbf{r}} \rightarrow \frac{1}{4} \sum_{\mathbf{r}'/\mathbf{r}} \phi_{\mathbf{r}'}(t)$ is the average neighboring field of site \mathbf{r} , and the sum is over the 4 first nearest-neighbors sites \mathbf{r}' of site \mathbf{r} . If the flip happens, $\phi_{\mathbf{r}}$ changes by $-2s/\Omega$, thus its average change in time is given by the rate equation

$$\frac{\partial \phi_{\mathbf{r}}(t)}{\partial t} = [1 - \phi_{\mathbf{r}}(t)] P(- \rightarrow +) - [1 + \phi_{\mathbf{r}}(t)] P(+ \rightarrow -), \quad (47)$$

where the first (second) term corresponds to a $- \rightarrow +$ ($+ \rightarrow -$) flip event. In order to obtain a closed equation for ϕ (see Appendix A for details), we substitute the expression for the transition probabilities Eq. (46) into Eq. (47), we then expand around $\psi_{\mathbf{r}} = 0$, and replace the neighboring field $\psi_{\mathbf{r}}$ by $\phi_{\mathbf{r}} + \Delta\phi_{\mathbf{r}}$, where Δ is defined as the standard Laplacian operator $\Delta\phi_{\mathbf{r}} \equiv \frac{1}{4} \sum_{\mathbf{r}'/\mathbf{r}} (\phi_{\mathbf{r}'} - \phi_{\mathbf{r}}) = \psi_{\mathbf{r}} - \phi_{\mathbf{r}}$. Keeping the expansion up to first order in $\Delta\phi_{\mathbf{r}}$, results in the following equation for the spin field

$$\begin{aligned} \frac{\partial \phi_{\mathbf{r}}(t)}{\partial t} = & 2^{-a} (1 - \phi_{\mathbf{r}}^2) \left[v + (a-1)\phi_{\mathbf{r}} + \frac{v}{2}(a-1)(a-2)\phi_{\mathbf{r}}^2 \right. \\ & \left. + \frac{1}{6}(a-1)(a-2)(a-3)\phi_{\mathbf{r}}^3 \right] \\ & + 2^{-a} a \left[1 + v(a-2)\phi_{\mathbf{r}} + \frac{1}{2}(a-1)(a-4)\phi_{\mathbf{r}}^2 \right] \Delta\phi_{\mathbf{r}}. \end{aligned} \quad (48)$$

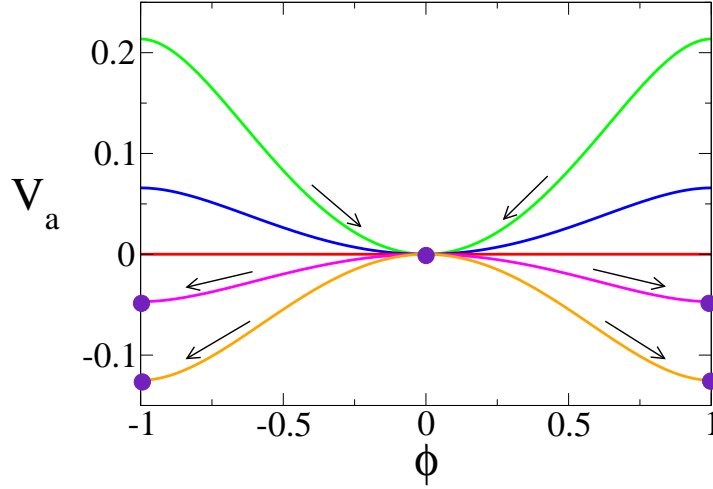


Figure 9. Ginzburg-Landau potential Eq. (52) for the symmetric case $v = 0$ of the Abrams-Strogatz model, with volatility values $a = 0.5, 0.8, 1.0, 1.2$ and 2.0 (from top to bottom). For $a = 0.5$ and 0.8 the system relaxes to an active state with the same fraction of up and down spins uniformly distributed over the space, corresponding to the minimum of the potential at $\phi = 0$, while for $a = 1.2$ and 2.0 it reaches full order, described by the field $|\phi| = 1$.

Equation (48) can be written in the form of a time dependent Ginzburg-Landau equation

$$\frac{\partial \phi_{\mathbf{r}}(t)}{\partial t} = D(\phi_{\mathbf{r}}) \Delta \phi_{\mathbf{r}} - \frac{\partial V_{a,v}(\phi_{\mathbf{r}})}{\partial \phi_{\mathbf{r}}}, \quad (49)$$

with diffusion coefficient

$$D(\phi_{\mathbf{r}}) \equiv 2^{-a} a \left[1 + v(a-2)\phi_{\mathbf{r}} + \frac{1}{2}(a-1)(a-4)\phi_{\mathbf{r}}^2 \right] \quad (50)$$

and potential

$$\begin{aligned} V_{a,v}(\phi_{\mathbf{r}}) \equiv 2^{-a} \left\{ -v\phi_{\mathbf{r}} - \frac{1}{2}(a-1)\phi_{\mathbf{r}}^2 + \frac{v}{6} [2 - (a-1)(a-2)] \phi_{\mathbf{r}}^3 \right. \\ \left. + \frac{1}{24}(a-1) [6 - (a-2)(a-3)] \phi_{\mathbf{r}}^4 + \frac{v}{10}(a-1)(a-2)\phi_{\mathbf{r}}^5 \right. \\ \left. + \frac{1}{36}(a-1)(a-2)(a-3)\phi_{\mathbf{r}}^6 \right\}, \quad (51) \end{aligned}$$

which is analogous to the potential for the global magnetization m in the fully connected network case (Fig. 4). As we already discussed in section 2.1, for the asymmetric case $v \neq 0$ the ordering dynamics is strongly determined by v . When $a > 1$, $V_{a,v}$ has the shape of a double-well potential with minima at $\phi = \pm 1$, and with a well deeper than the other, thus the system is quickly driven by the bias towards the lowest minimum, reaching full order in a rather short time. For $a < 1$ there is a minimum at $|\phi| < 1$, thus the system relaxes to a partially ordered state of language coexistence composed by a well mixed population with different proportions of speakers of the two languages.

Specially interesting is the analysis of the symmetric case $v = 0$, for which the potential is (see Fig. 9)

$$V_a(\phi_{\mathbf{r}}) = 2^{-a}(a-1) \left\{ -\frac{\phi_{\mathbf{r}}^2}{2} + [6 - (a-2)(a-3)] \frac{\phi_{\mathbf{r}}^4}{24} + (a-2)(a-3) \frac{\phi_{\mathbf{r}}^6}{36} \right\}. \quad (52)$$

In this bias-free case, when $a < 1$ the minimum is at $\phi = 0$, thus the average magnetization in a small region around a given point \mathbf{r} is zero, indicating that the system remains disordered (language coexistence). This can be seen in Fig. 10(b), where we show a snapshot of the lattice for the model with $v = 0$ and $a = 0.5$, after it has reached a stationary configuration. For $a > 1$ the potential has two wells with minima at $\phi = \pm 1$, but with the same depth, thus there is no preference for any of the two states, and the system orders in either of the language dominance states by spontaneous symmetry breaking. The order-disorder nonequilibrium transition at $a = 1$ is reminiscent of the well known Ising model transition, but with the volatility parameter a playing the role of temperature: high volatility $a < 1$ corresponds to the high temperature paramagnetic phase and low volatility to the low temperature phase. An important difference is that the transition is here first order, since the low volatility stable states $\phi = \pm 1$ appear discontinuously at $a = 1$. In addition, while in the low temperature phase of the Ising model, spins flip in the bulk of ordered domains by thermal fluctuations, here, spin flips in the low volatility regime only occur at the interfaces (domain boundaries).

Complete ordering for $a > 1$ is achieved through domain coarsening driven by surface tension [32]. That is, as the system evolves, same-spin domains are formed, small domains tend to shrink and disappear while large domains tend to grow. Figure 10(d) shows a snapshot of the lattice for the evolution of the model with $a = 2$. We observe that domains have rounded boundaries given that the dynamics tends to reduce their curvature, leading to an average domain length that grows with time as $l \sim t^{1/2}$ [16, 24]. For the special case $a = 1$ (voter model) the potential is $V_a = 0$, there is still coarsening but without surface tension, meaning that domain boundaries are driven by noise, as seen in Fig. 10(c). As a consequence of this, the average length of domains grows very slowly with time, as $l \sim \ln t$ [33, 34, 35].

In order to compare the behavior of the language competition models described before in fully connected and complex networks with their behavior in square lattices we have numerically explored the stability regions in the (a, v) plane for the ASM and BM in square lattices. The coexistence-dominance transition in the ASM for $v = 0$ is at $a_c \simeq 1.0$, as in fully connected and complex networks, whereas the region for coexistence is found to be much more narrow than the ones observed in complex networks with low degree, like the one depicted in Fig. 6 for $\mu = 3$. Using the simulation applet [31] one can check that for a given value of $v \neq 0$, the disordered stationary state that characterizes coexistence is harder to maintain in square lattices than in random networks: in order to have an equivalent situation, a smaller value of a is needed in the former case.

In the BM, apart from the narrowing of the coexistence region, we also found that the transition point for $v = 0$ is shifted to an even smaller value of the volatility a than

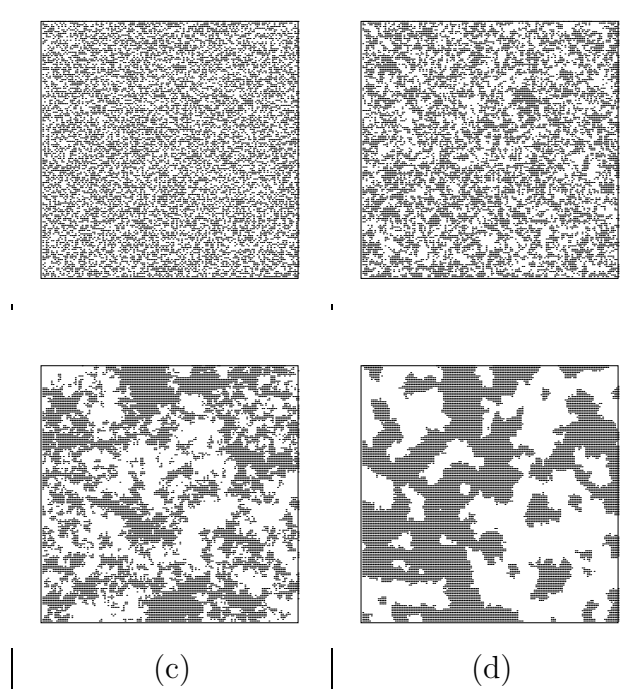


Figure 10. Snapshots of the Abrams-strogatz model with bias $v = 0$ on a 128×128 square lattice and three values of volatility, $a = 0.5$ (b), $a = 1.0$ (c) and $a = 2.0$ (d). (a) Initial state: each site is occupied with a spin $+1$ or -1 with the same probability $1/2$. (b) The system reaches an active disordered stationary state, with a global magnetization that fluctuates around zero. (c) The system displays coarsening driven by noise, characterized by domains with noisy boundaries. (d) There is also coarsening but driven by surface tension, generating domains with more rounded boundaries.

in complex networks. To see this, in Fig. 11 we show the time evolution of the inverse of the average interface density $\langle \rho \rangle$ ‡ for various values of a , on a square lattice of size $N = 400^2$. We observe that $\langle \rho \rangle$ decays to zero for values of $a > 0.16$, indicating that the system orders (dominance phase), while $\langle \rho \rangle$ approaches to a constant value larger than zero for $a < 0.16$, thus the system remains disordered (coexistence phase). At the transition point $a_{sl} \simeq 0.16$ we have that $\langle \rho \rangle \sim 1/\ln(t)$, indicating that the transition belongs to the Generalized Voter class, a typical transition observed in spin systems with two symmetric absorbing states [25, 26, 36, 37].

The fact that $a_{sl} \simeq 0.16$ is smaller than the corresponding transition points $a_{fc} \simeq 0.63$ and $a_{cn} \simeq 0.3$, together with the narrowing effect mentioned above, leads to the result that the region for coexistence is largely reduced in square lattices, compared to fully connected and complex networks.

‡ The $\langle \dots \rangle$ indicates average over independent realizations of the dynamics with different random initial conditions.

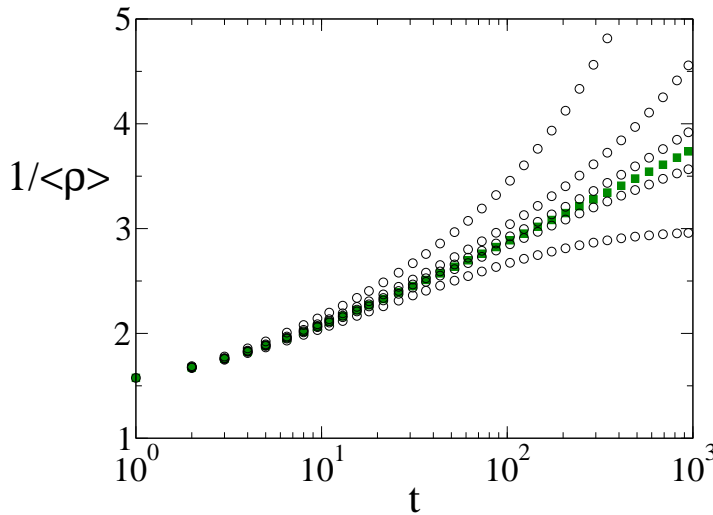


Figure 11. Inverse of the average interface density $\langle \rho \rangle$ vs time, on a log-linear scale, for the Bilinguals model. From top to bottom: $a = 0.30, 0.20, 0.17, 0.16, 0.15$ and 0.10 . Averages were done over 10^3 independent realizations on a square lattice of side $L = 400$. $\langle \rho \rangle$ decays as $1/\ln(t)$ at the transition point $a_{sl} \simeq 0.16$ (solid squares), corresponding to the behavior of a Generalized voter transition in two dimensions.

5. Summary and conclusions

We have discussed the order-disorder transitions that occur in the volatility-prestige parameter space of two related models of language competition dynamics, the Abrams-Strogatz and its extension to account for bilingualism: the Bilinguals Model. We have analyzed their microscopic dynamics on fully connected, complex random networks and two-dimensional square lattices and constructed macroscopic descriptions of these dynamics accounting for the observed transitions. At a general level, we have found that both models share the same qualitative behavior, showing a transition from coexistence to dominance of one of the languages at a critical value of the volatility parameter a_c . The fact that agents are highly volatile ($a < a_c$), i.e, loosely attached to the language they are currently using, leads to the enhancement of language coexistence. On the contrary, in a low volatility regime ($a > a_c$), the final state is one of dominance/extinction.

A more detailed comparison of both models shows important differences: In the mean field description for fully connected networks, and for the ASM, a scenario of coexistence is obtained for $a < 1$. This is independent of the relative prestige of the languages, v . However, the stationary fraction of agents in the more prestigious language increases with a higher prestige. But when bilingual agents are introduced (BM), the scenario of coexistence becomes the parameter space area corresponding to $a < 0.63$. That is, the area of coexistence is reduced: agents with a higher level of volatility (smaller a) are needed in order to obtain a coexistence regime. Within this current framework, allowing the agents to use two languages at the same time, which is reasonable from a

sociolinguistic point of view, has the effect of making language coexistence more difficult to achieve, in the sense that coexistence occurs for a smaller range of parameters.

Network topology and local effects have been addressed through pair approximations for degree uncorrelated networks. For the ASM on degree-regular random networks we find that the decrease of the network connectivity leads to a reduction, in the parameter space (a, v) , of the area of language coexistence and the area of bistable dominance, while monostable dominance regions appear, in which only the state of dominance of the more prestigious language is stable. To gain intuition on this result, we first notice that in the fully connected network, the area of coexistence ($a < 1$) corresponds to a situation in which the majority of the agents use the more prestigious language. The fact that all agents are interconnected, translates to a situation in which users of the less prestigious language (minority) are in contact with every other agent in the network. In this situation, high volatility (agents switching their language use easily) is effective in order to achieve a steady state situation with individuals continuously changing the use of their language and making coexistence possible. In contrast, when considering a degree-regular random network, that is, when limiting the number of neighbors in a society, the existence of bias ($v \neq 0$) opens the possibility for agents in the majority language to be placed in domains without contact with the minority language. For a region of the parameter space where there is coexistence in a fully connected network, these domains can grow in size in a random network until they occupy the entire system. This gives rise to the monostable region of dominance of the more prestigious language found in complex networks with low connectivity. Compared to the fully connected case, a higher volatility is needed in order to overcome this topological effect, leading to a reduction of the area of coexistence. In two dimensional square lattices the coexistence is shown to be even more difficult to achieve, probably due to the fact that correlations with second neighbors make the coarsening process of formation and growth of domains easier. The macroscopic field description introduced for square lattices accounts for the different coarsening processes observed for large and small volatility.

The network effects described above for the ASM are also qualitatively valid for the BM. However, the reduction of the area of language coexistence is more important when considering bilingual agents. We find a shift of the critical value with the topology: $a_{fc} \simeq 0.63$ in fully connected networks, $a_{cn} \simeq 0.3$ in complex uncorrelated networks, and $a_{sl} \simeq 0.16$ in two dimensional square lattices.

In summary, building upon previous works on language competition [5, 14, 15], we have studied numerically and by analytical macroscopic descriptions, two microscopic models for the dynamics of language competition. We have analyzed the role of bilingual agents and social network structure in the order-disorder transitions occurring for different values of the two parameters of the models: the relative prestige of the languages and the volatility of the agents. We have found that the scenario of coexistence of the two languages is reduced when bilingual agents are considered. This reduction also depends on the social structure, with the region of coexistence shrinking when the connectivity of the network decreases.

We acknowledge support from project FISICOS (FIS2009-60327) of MEC and FEDER, and from NEST-Complexity project PATRES (043268).

- [1] C. Castellano, S. Fortunato, and V. Loreto. Statistical physics of social dynamics. *Reviews of Modern Physics*, 81:591, 2009.
- [2] M. San Miguel, V.M. Eguíluz, R. Toral, and K. Klemm. Binary and multivariate stochastic models of consensus formation. *Computer in Science and Engineering*, 7:67–73, 2005.
- [3] R. Appel and P. Muysken. *Language Contact and Bilingualism*. Edward Arnold Publishers, London, 1987.
- [4] J. Mira and A. Paredes. Interlinguistic similarity and language death dynamics. *Europhysics Letters*, 69:1031–1034, 2005.
- [5] D. M. Abrams and S. H. Strogatz. Modelling the dynamics of language death. *Nature*, 424:900, 2003.
- [6] D. Crystal. *Language death*. Cambridge University Press, Cambridge, 2000.
- [7] D. Stauffer, X. Castelló, V. M. Eguíluz, and M. San Miguel. Microscopic abrams-strogatz model of language competition. *Physica A*, 374:835–842, 2007.
- [8] M. Patriarca and E. Heinsalu. Influence of geography on language competition. *Physica A*, 388:174–186, 2009.
- [9] J.P. Pinasco and L. Romanelli. Coexistence of languages is possible. *Physica A*, 361(1):355–360, February 2006.
- [10] C. Schulze and D. Stauffer. Monte carlo simulation of the rise and the fall of languages. *International Journal of Modern Physics C*, 16(5):781–787, 2005.
- [11] Viviane M. de Oliveira, M.A.F. Gomes, and I.R. Tsang. Theoretical model for the evolution of the linguistic diversity. *Physica A*, 361(1):361–370, February 2006.
- [12] T. M. Liggett. *Interacting Particle Systems*. New York: Springer, 1985.
- [13] J. Marro and R. Dickman. *Nonequilibrium Phase Transitions in Lattice Models*. Cambridge University Press: Cambridge, U.K., 1999.
- [14] William S-Y. Wang and James W. Minett. The invasion of language: emergence, change and death. *Trends in Ecology and Evolution*, 20:263–269, 2005.
- [15] J. W. Minett and W. S.-Y. Wang. Modelling endangered languages: The effects of bilingualism and social structure. *Lingua*, 118:19–45, 2008.
- [16] X. Castelló, V. M. Eguíluz, and M. San Miguel. Ordering dynamics with two non-excluding options: bilingualism in language competition. *New Journal of Physics*, 8:308–322, 2006.
- [17] X. Castelló, R. Toivonen, V. M. Eguíluz, J. Saramäki, K. Kaski, and M. San Miguel. Anomalous lifetime distributions and topological traps in ordering dynamics. *Europhysics Letters*, 79:66006 (1–6), 2007.
- [18] R. Toivonen, X. Castelló, V. M. Eguíluz, J. Saramäki, K. Kaski, and M. San Miguel. Broad lifetime distributions for ordering dynamics in complex networks. *Physical Review E*, 79:016109, 2008.
- [19] L. Dall’Asta and C. Castellano. Effective surface-tension in the noise-reduced voter model. *Europhysics Letters*, 77:60005, 2007.
- [20] H. U. Stark, C. J. Tessone, and F. Schweitzer. Slower is faster: Fostering consensus formation by heterogeneous inertia. *Advances in Complex Systems*, 11:551, 2008.
- [21] R. A. Blythe. Generic modes of consensus formation in stochastic language dynamics. *Journal of Statistical Mechanics*, P02059, 2009.
- [22] F Vazquez, P L Krapivsky, and S Redner. Constrained opinion dynamics: freezing and slow evolution. *J. Phys. A: Math. Gen.*, 36:L61–L68, 2003.
- [23] F Vazquez, , and S Redner. Ultimate fate of constrained voters. *J. Phys. A: Math. Gen.*, 37:8479–8494, 2004.
- [24] L. Dall’Asta and T. Galla. Algebraic coarsening in voter models with intermediate states. *J. Phys. A: Math. Theor.*, 41:435003, 2008.
- [25] O. Al Hammal, H. Chaté, I Dornic, and M. A. Muñoz. Langevin description of critical phenomena

- with two symmetric absorbing states. *Physical Review Letters*, 94:230601, 2005.
- [26] F. Vazquez and C. López. Systems with two symmetric absorbing states: relating the microscopic dynamics with the macroscopic behavior. *Phys. Rev. E*, 78(061127), 2008.
- [27] F. Vazquez and V. M. Eguiluz. Analytical solution of the voter model on uncorrelated networks. *New Journal of Physics*, 10(063011), 2008.
- [28] P. Erdős and A. Rényi. On the evolution of random graphs. *Publ.Math. (Debrecen)*, 6:290–297, 1959.
- [29] A.-L. Barabási and R. Albert. Emergence of scaling in random networks. *Science*, 286:509, 1999.
- [30] E. Pugliese and C. Castellano. Heterogeneous pair approximation for voter models on networks. *Europhysics Letters*, 88:58004 (1–6), 2009.
- [31] X. Castelló. Dynamics of language competition. From IFISC website: http://www.ifisc.uib-csic.es/research/complex/APPLET_LANGDYN.html, 2007.
- [32] J. D. Gunton, M. San Miguel, and P. Sahní. *Phase Transitions and Critical Phenomena*, volume 8, chapter The dynamics of first order phase transitions, pages 269–446. Academic Press, London, 1983.
- [33] P. L. Krapivsky. Kinetics of monomer-monomer surface catalytic reactions. *Phys. Rev. A*, 45(2):1067–1072, Jan 1992.
- [34] L. Frachebourg and P. L. Krapivsky. Exact results for kinetics of catalytic reactions. *Physical Review E*, 53:R3009, 1996.
- [35] Sidney Redner. *A Guide to First-Passage Processes*. Cambridge University Press, August 2001.
- [36] I. Dornic, H. Chaté, J. Chave, and H. Hinrichsen. Critical coarsening without surface tension: The universality class of the voter model. *Physical Review Letters*, 87:045701, 2001.
- [37] M. Droz, A. L. Ferreira, and A. Lipowski. Splitting the voter potts model critical point. *Physical Review E*, 67:056108, 2003.

Appendix A. Equation for the spin field $\phi_{\mathbf{r}}$

In this section we shall derive an equation for the spin field $\phi_{\mathbf{r}}$. We start by substituting the expression for the transition probabilities Eq. (46) into Eq. (47) and by writing it in the more convenient form

$$\frac{\partial \phi}{\partial t} = \frac{(1+v)}{2^{a+1}}(1-\phi)(1+\psi)(1+\psi)^{a-1} - \frac{(1-v)}{2^{a+1}}(1+\phi)(1-\psi)(1-\psi)^{a-1}, \quad (\text{A.1})$$

where ϕ and ψ are abbreviated forms of $\phi_{\mathbf{r}}$ and $\psi_{\mathbf{r}}$ respectively. We now replace the neighboring field ψ in the terms $(1+\psi)$ and $(1-\psi)$ of Eq. (A.1) by $\psi \equiv \phi + \Delta\phi$, where Δ is defined as the standard Laplacian operator $\Delta\phi_{\mathbf{r}} \equiv \frac{1}{4} \sum_{\mathbf{r}'/\mathbf{r}} (\phi_{\mathbf{r}'} - \phi_{\mathbf{r}}) = \psi_{\mathbf{r}} - \phi_{\mathbf{r}}$, and obtain

$$\begin{aligned} \frac{\partial \phi}{\partial t} = & 2^{-(a+1)}(1-\phi^2) [(1+v)(1+\psi)^{a-1} - (1-v)(1-\psi)^{a-1}] \\ & + 2^{-(a+1)} [(1+v)(1-\phi)(1+\psi)^{a-1} + (1-v)(1+\phi)(1-\psi)^{a-1}] \Delta\phi. \end{aligned} \quad (\text{A.2})$$

Because our idea is to obtain a Ginzburg-Landau equation with a ϕ^6 -potential, the right hand side of Eq. (A.3) must be proportional to ϕ^5 , and therefore we use the Taylor series expansions around $\psi = 0$

$$\begin{aligned} (1 \pm \psi)^{a-1} &= 1 + (a-1)\psi + \frac{1}{2}(a-1)(a-2)\psi^2 + \frac{1}{6}(a-1)(a-2)(a-3)\psi^3 \quad \text{and} \\ (1 - \psi)^{a-1} &= 1 - (a-1)\psi + \frac{1}{2}(a-1)(a-2)\psi^2 - \frac{1}{6}(a-1)(a-2)(a-3)\psi^3 \end{aligned}$$

into Eq. (A.3), to obtain

$$\begin{aligned} \frac{\partial \phi}{\partial t} = & 2^{-a}(1-\phi^2) \left[v + (a-1)\psi + \frac{v}{2}(a-1)(a-2)\psi^2 + \frac{1}{6}(a-1)(a-2)(a-3)\psi^3 \right] \\ & + 2^{-a} \left\{ (1-v\phi) \left[1 + \frac{1}{2}(a-1)(a-2)\psi^2 \right] \right. \\ & \left. + (v-\phi) \left[(a-1)\psi + \frac{1}{6}(a-1)(a-2)(a-3)\psi^3 \right] \right\} \Delta\phi. \end{aligned} \quad (\text{A.3})$$

We then replace ψ by $\phi + \Delta\phi$ in Eq. (A.3) and expand to first order in $\Delta\phi$, assuming that the field ϕ is smooth, so that $\Delta\phi \ll \phi$. Finally, neglecting ϕ^3 and higher order terms in the diffusion coefficient that multiplies the laplacian, we arrive to the expression for the spin field quoted in Eq. (48).